

POLYCRYSTALLINE FILMS OF PHOSPHORS $\text{Cd}_{(1-x-y-z)}(\text{Cu}_y\text{Ag}_z)\text{Zn}_x\text{S}$ ON THE SILICON SUBSTRATE WITH THE SILICON CARBIDE BUFFER LAYER: STRUCTURE AND PROPERTIES

N.M. Sergeeva¹, S.P. Bogdanov¹, A.V. Redkov²

¹St. Petersburg State Technological Institute (Technical University) (SPbSTI (TU)) 190013, St. Petersburg,
Moskovsky pr. 26, Russia

²ITMO University, 197101, St. Petersburg, Kronverkskiy pr., 49, Russia

*e-mail: alnserg41@mail.ru

Abstract. Polycrystalline phosphor film $\text{Cd}_{(1-x-y-z)}(\text{Cu}_y\text{Ag}_z)\text{Zn}_x\text{S}$ was grown on the surface of the Si/nano-SiC heterostructure obtained by the unique method of substitution of atoms. The structural, phonon (vibrational) properties of the film, as well as its morphology were studied. X-ray phase analysis (XRD) showed that the phase composition is represented by a matrix of solid solution of cubic syngony and impurity phases formed during precipitation: sodium sulfate (Na_2SO_4) of orthorhombic syngony and sodium cadmium sulfide ($\text{Na}_6\text{Cd}_7\text{S}_{10}$) of monoclinic syngony. The Raman spectroscopy (RS) method confirmed the components of the polycrystalline phosphor film, including its phase composition, determined by the X-ray phase analysis method.

Keywords: phosphor, $\text{Cd}_{1-x}\text{Zn}_x\text{S}$, copper, silver, polycrystalline film, Si/(nano)SiC heterostructures, Raman spectroscopy

1. Introduction

We have previously studied the optical properties of phosphors based on the three-component solid solution $\text{Cd}_{(1-x-y-z)}(\text{Cu}_y\text{Ag}_z)\text{Zn}_x\text{S}$ in the visible region of the energy spectrum of photons exciting valence electrons in the range from 3.1 eV to ~ 1.6 eV [1,2]. It is known [2-5] that phosphors based on a solid solution of zinc sulfides and cadmium are characterized by higher electrical, optical properties and variable color characteristics unlike luminescent substances based on individual zinc or cadmium sulfides under identical synthesis conditions. However, researchers were constantly interested in what controls the properties of crystals: phonons, phonon-electron interaction, or in other words, the interaction of light quanta and lattice thermal energy, translational symmetry, anisotropy?

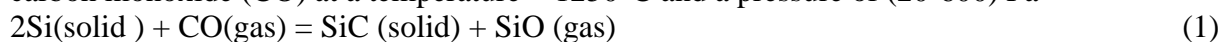
In this connection, the solid solutions of $\text{Cd}_{(1-x)}\text{Zn}_x\text{S}$ compounds A^2B^6 attract the attention of researchers with their structural features for a wide application, including for solar cells McPeak [6], as luminescent substances [2]. Perspective are the phosphors obtained by the method of colloid chemistry. Synthesis and simultaneous doping it, for example, with two ions, copper and silver, causes a decrease in the crystallographic symmetry of the cubic lattice of the matrix solid solution $\text{Cd}_{1-x}\text{Zn}_x\text{S}$. The broadening of the photoluminescence spectrum of doped solid solutions is observed in the long-wave region of radiation.

Copper and silver make it possible to obtain a white luminescence and increase the intensity of its emission by a factor of two at a wavelength of 500 nm in comparison with an undoped solid solution. Therefore, an interesting and promising study would be the study of

the phonon properties of phosphor films deposited on single-crystal substrates and, in particular, on a silicon substrate (Si) with a buffer layer (sublayer) of silicon carbide (SiC). The combination of unique optical properties of solid solutions of ZnS-CdS sulfides with Si properties can lead to the creation of a whole class of devices of new generation.

The study of the vibrational properties of the structure of solid solutions will broaden our knowledge of the optical properties of the polycrystalline phosphor film on a silicon substrate with a buffer nanolayer of silicon carbide.

Thin silicon carbide (SiC) films on a monocrystalline silicon (Si) substrate were grown by a new method of topochemical substitution of atoms. This substitution method was discovered by S.A. Kukushkin and A.V. Osipov in 2008 [7-11]. According to this method, the growth of single-crystal SiC on a silicon substrate is due to the chemical reaction (1) of Si and carbon monoxide (CO) at a temperature $\sim 1250^\circ\text{C}$ and a pressure of (20-600) Pa



Azhniuk [12] studied the Raman spectra of nanocrystals of solid solutions Cd_{1-x}Zn_xS ($x = 0 \dots 0.13$) in borosilicate glass. The excitation was carried out by the laser line Ag⁺ at a wavelength $\lambda = 457.9$ nm. The Raman spectra of the solid solutions Cd_{1-x}Zn_xS ($x = 0 \dots 0.13$) are given. Moreover, as the value of x increases, the main peaks shift to a region of high frequencies, that is, the blue shift. The Raman spectrum of cadmium sulfide (CdS) is represented by two optical frequencies at 305 and 612 cm⁻¹.

However, despite attention to the phosphors based on solid solutions of zinc and cadmium sulfides, their phonon properties have not been fully studied, despite the fact that the phonon properties of these crystal structures can provide important information about the dynamics of the crystal lattice and explain many of the physicochemical properties, including optical, of luminescent materials.

Therefore, the aim of this work was to study the fine structure, phase composition, structural, phonon properties, and morphology of the surface of a polycrystalline Cd_(1-x)Zn_(x)S: Cu, Ag phosphor film deposited from an aqueous colloidal solution onto the surface of the heterostructure Si/(nano)SiC.

2. Experimental

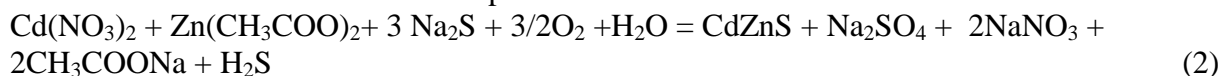
Technique of the experiment. The following reagents were used to synthesize the basis of phosphors: zinc acetate dihydrate (Zn(CH₃COO)₂·2H₂O, cadmium nitrate tetrahydrate Cd(NO₃)₂·4H₂O, ninehydrate sodium sulfide Na₂S·9H₂O and bidistilled water. The calculated amount of copper and silver activators was introduced as the corresponding salts of Cu(CH₃COO)₂·H₂O and AgNO₃. Copper and silver were introduced in the synthesis in amounts of 0.02 and 0.06 (g/g_{Cd0.1Zn0.9S}), respectively. The investigated reagents had the qualification "analytical grade".

Colloidal precipitation of sulfides was carried out in two stages. In the first stage, aqueous solutions of zinc acetate and cadmium nitrate containing copper (in the form of acetate), silver (in the form of a nitrate salt), and a solution of sodium sulfide (metal precipitant) were prepared. Solutions of zinc acetate, cadmium nitrate and sodium sulfide had a concentration of 1 mol/l. In the second stage, precipitation and doping of zinc and cadmium sulfides were carried out.

The colloidal aqueous solution was then divided into two parts. In one part, after separation of the precipitate from the solution and vacuum drying (starting sample 2), a crystalline precipitate was obtained and its optical and structural characteristics were studied. Another part of the colloidal solution was used to grow a film on the surface of a silicon substrate with a nano-SiC (111) buffer layer by the free precipitation of zinc acetate, cadmium nitrate, copper acetate, silver nitrate, sodium sulfide. To this end, hybrid Si/nano-SiC substrates were placed in a Petri dish, a certain amount of a colloidal aqueous phosphor

solution was added and kept in solution until all the particles were completely deposited on the surface of the substrate. The deposition of the film was carried out under normal conditions.

The main reaction of colloid deposition of cadmium and zinc sulfides:



Further, after drying the phosphor film on the substrate, the phase composition, structural characteristics, surface morphology, elemental and disperse composition were studied. Determination of the elemental composition of the samples was carried out by electron-probe microanalysis. The sensitivity of the method was 0.1at.%.

For X-ray phase analysis (XRD), a micro diffractometer "Difrey" was used. Diffraction patterns were measured in a range of angles 2θ 10 ... 70° in a discrete mode with a step $\Delta 2\theta = 0.040$ and exposure time 1s, using Cu-K $_{\alpha}$ radiation at a wavelength of $\lambda = 0.1542$ nm. Identification of the phase composition of the sediment was carried out according to the file of the International Center for Diffraction Data (PDF card).

Raman spectra were measured using a confocal Raman microscope Witec Alpha 300R with a sensitive optical CCD detector at room temperature. The measurements were performed in the backscattering geometry z (xx) \bar{z} and in the phonon oscillation range 100-3600 cm^{-1} (or the wavelengths of the radiation in the infrared region of the spectrum of 10^5 nm - $2.8 \cdot 10^3$ nm and energies ~ 0.01 - 0.44 eV). The output power of laser radiation is 1 mW, the optical excitation wavelength is $\lambda = 532$ nm, (photon energy of 2.33 eV) in the green region of the electromagnetic spectrum.

XRD analysis. Figure 1 shows the diffractogram of the resulting phosphor $\text{Cd}_{0.1}\text{Zn}_{0.9}\text{S}$, on which impurity reflections are also observed. Also in Fig. 1 shows the diffraction patterns of sodium sulfate (Na_2SO_4) standards (PDF card: 05-0631), sodium cadmium sulfide ($\text{Na}_6\text{Cd}_7\text{S}_{10}$) (PDF card: 51-1427). The reflexes corresponding to the impurity phases of Na_2SO_4 and $\text{Na}_6\text{Cd}_7\text{S}_{10}$ were designated, respectively, by triangles and circles. The impurity phases: Na_2SO_4 orthorhombic system $Fddd$ (PDF card: 05-0631) and $\text{Na}_6\text{Cd}_7\text{S}_{10}$ monoclinic $C2/m$ (PDF card: 51-1427) were identified by the values of the interplanar spacings d (Fig. 1 and Table 1).

As can be seen from Table 1, the correspondence between the reference interplanar distances confirms the formation of impurity phases in the phosphor obtained by colloidal deposition: sodium sulfate (Na_2SO_4) and sodium cadmium sulfide ($\text{Na}_6\text{Cd}_7\text{S}_{10}$).

Table 2 shows the values of the parameters of the crystal cubic lattice of the standards Si, 3C-SiC, solid solution $\text{Cd}_{0.1}\text{Zn}_{0.9}\text{S}$, and the synthesized phosphor based on it.

As can be seen from Table 2, the standards of Si and the solid solution $\text{Cd}_{0.1}\text{Zn}_{0.9}\text{S}$ are close in terms of the parameters of the cubic crystal lattice. Spatial groups or the crystallographic environment of atoms in Si and $\text{Cd}_{0.1}\text{Zn}_{0.9}\text{S}$ lattices in the crystal structure of $Fd-3m$ and $F\bar{4}3m$ (T_d^2), respectively.

In addition to the similarity of silicon crystal and solid solution in terms of syngony, both types of crystals are similar in the same three-layer structural motif, a rotary axis of the third order, a symmetry plane parallel to the diagonal of the face. Therefore, it was assumed that the correspondence of the crystal lattices of silicon and a solid solution would allow the formation of phosphor films without elastic stresses.

The energy brightness of the PL of the phosphor $\text{Cd}_{(1-x-y-z)}(\text{Cu}_y\text{Ag}_z)\text{Zn}_{(x)}\text{S}$ increased 3.5 times after deposition onto the substrate of the Si/(nano) SiC heterostructure. The energy brightness of the phosphor before and after aging in an aqueous colloidal solution is 18 and 64 cd/m^2 , respectively.

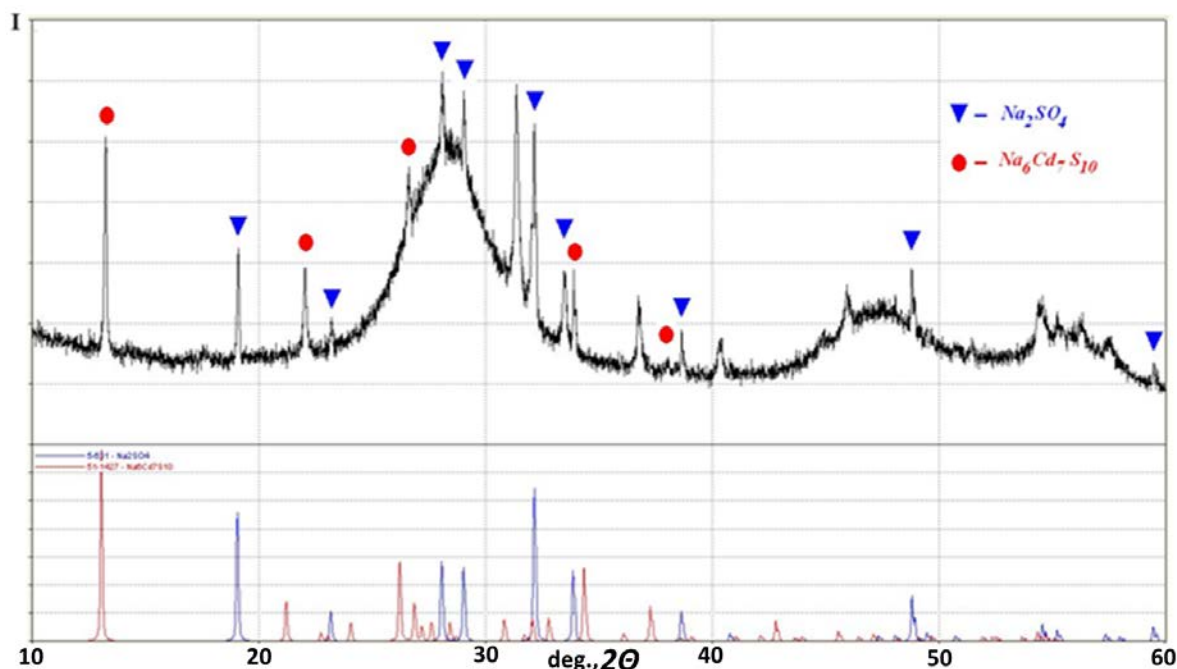


Fig. 1. Diffraction patterns of the Cd_(1-x-y-z)(Cu_yAg_z)Zn_xS phosphor and standards: sodium sulfate (Na₂SO₄) (PDF card: 05-0631), sodium cadmium sulfide (Na₆Cd₇S₁₀) (PDF card: 51-1427)

Table 1. Indication of the impurity phases: Na₂SO₄ and Na₆Cd₇S₁₀ in the Cd_(1-x-y-z)(Cu_yAg_z)Zn_xS phosphor by comparing the experimental data and the standards of the PDF card

| PDF card, formula, syngony, space group, coordination number, Z | | Experiment |
|--|---------------------------------|-----------------------|
| hkl | d _{hkl} , nm(PDF card) | d _{hkl} , nm |
| PDF card: 05-0631: Na ₂ SO ₄ orthorhombic Fddd; Z=8 | | |
| 111 | 0.4660 | 0.4541 |
| 131 | 0.3178 | 0.3177 |
| 040 | 0.3075 | 0.3072 |
| 113 | 0.2783 | 0.2784 |
| 220 | 0.2646 | 0.2643 |
| 222 | 0.2329 | 0.2328 |
| 153 | 0.1864 | 0.1865 |
| 260 | 0.1680 | 0.1681 |
| PDF card: 51-1427: Na ₆ Cd ₇ S ₁₀ monoclinic C 2/m; Z=2 | | |
| 201 | 0.6790 | 0.6691 |
| 112 | 0.3110 | 0.3072 |

| | | |
|-----|--------|--------|
| 312 | 0.2820 | 0.2851 |
| 710 | 0.2730 | 0.2675 |
| 711 | 0.2487 | 0.2444 |

Table 2. Parameters of the crystalline cubic lattice of silicon, silicon carbide and phosphor, experimental and reference (PDF card)

| Lattice parameter, nm | | | | |
|-----------------------|---------|---------------------------------------|---|--------------------|
| Si | 3C-SiC | Cd _{0,1} Zn _{0,9} S | Cd _(1-x-y-z) (Cu _y Ag _z)Zn _(x) S | |
| PDF card | | | Experiment | |
| 12-1402 | 73-1708 | 024- 1137 | aged in an aqueous colloidal solution (sample 1) | initial (sample 2) |
| 0.543 | 0.435 | 0.543 | 0.534 | 0.548 |

The growth of the energy brightness in the precipitation of Cd_(1-x-y-z)(Cu_yAg_z)Zn_(x)S was associated with the process of co-crystallization, during which crystals of one phase can nucleate on the surface of another phase, forming a system of heterojunctions. Axtell [13] synthesized and studied the physico-chemical properties of the ternary compound Na₆Cd₇S₁₀, since this compound has interesting structural features, including the number of vacancies and strange coordination geometry around the sulfur atom. It was shown that the triple compound Na₆Cd₇S₁₀ is a direct-gap semiconductor. Sodium cadmium sulfide (Na₆Cd₇S₁₀) has a tunneled three-dimensional framework, displays a sulfur atom in a rare coordination geometry and contains numerous built-in V_{Cd} cadmium vacancies. Such a structure is capable of initiating luminescent properties. However, we assume the role of phonon properties of the phosphor polycrystalline film in the enhancement of optical properties, including energy brightness.

Raman spectroscopy. The Raman analysis of the polycrystalline phosphor film on the substrate surface of a Si/nano-SiC heterostructure is shown in Fig. 2 and Table 3.

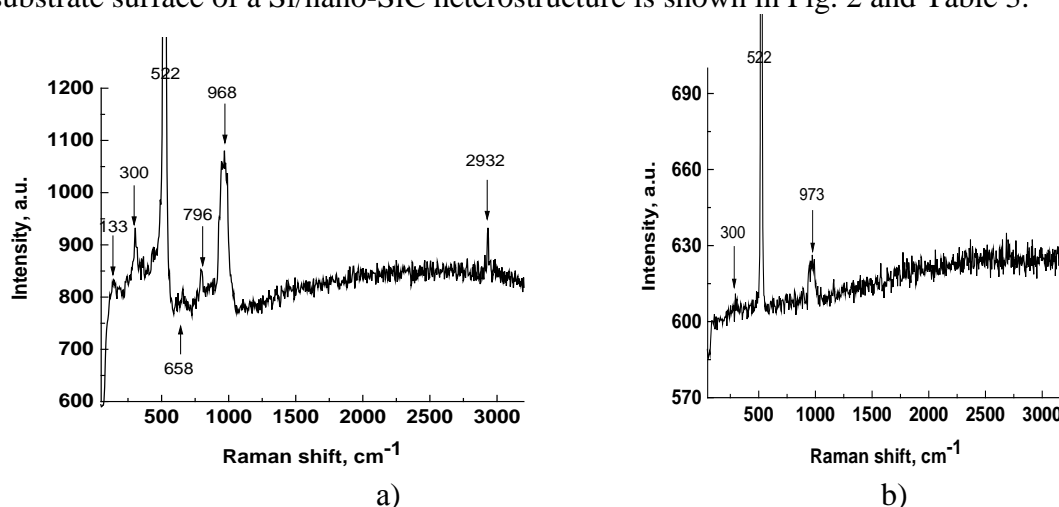


Fig. 2. Raman spectra: a) sections of a polycrystalline Cd_(1-x-y-z)(Cu_yAg_z)Zn_(x)S phosphor film on a silicon substrate with a nano silicon carbide film, and b) a silicon substrate with a nano silicon carbide film

Table 3. Indication of the Raman frequencies of a polycrystalline Cd_(1-x-y-z) (CuyAgz)Zn_xS phosphor film deposited on the surface of a Si/nano-SiC heterostructure

| Polycrystalline phosphor film Cd _(1-x-y-z) (CuyAgz) Zn _x S | |
|--|---|
| Frequency, cm ⁻¹ | Component and link |
| 133*, ** | LA 6H – SiC [14], LA SiC [7], [15]. |
| 300 | Si, (Si+CdS), Cd _{1-x} Zn _x S, CdS (~304 cm ⁻¹) [16], Si (520cm ⁻¹), CdS: 300 и 602 cm ⁻¹ [17], CdS: 305 и 612 cm ⁻¹ , Cd _{1-x} Zn _x S (x 0...0.13) in borosilicate glass. Anti-Stokes bias detected [12], CdS: 300 (1LO), 600 (2LO), 900(3LO) [18], (CdS + Si + solid solution Cd _{1-x} Zn _x S) [19], Si (~300 cm ⁻¹ и ~ 525 cm ⁻¹) [20]. |
| area 400 cm ⁻¹ : 332, 363, 395 | Zn _{1-x} Cd _x S: Cu,Cl (348 cm ⁻¹ : 1LO (345.4 cm ⁻¹) и 2LO (329.7 cm ⁻¹)). With increasing Cd (x > 0.1), the red shift is 1LO and 2LO (stokes shift). The modes of optical phonons: single-mode, intermediate and two-mode [21]. |
| 443 | |
| 522 | TO-Si crystal (521cm ⁻¹) and the low-frequency component near 480 cm ⁻¹ is associated with the amorphous phase [22]; p-Si (515...517 cm ⁻¹) confirmed [23, 24] and for clusters nc-Si в [25], c-Si (520.5 cm ⁻¹) [26]; Si (520 cm ⁻¹) [17] [27]; Si (520 cm ⁻¹ , 900 cm ⁻¹ – silicon substrate) [28]. |
| 612 ...625 depending on x | solid solution Cd _{1-x} Zn _x S x = 0...0.13, anti-Stokes shift with increasing x [12], but this frequency range is not detected on the Raman spectrum of the phosphor film. |
| 658 | solid solution [27], [29–33]. |
| 796 | TO 3C-SiC, TO 4H –SiC, TO 6 SiC (797cm ⁻¹) [14], 3C-SiC (on two frequencies: 796 и 972 cm ⁻¹) [15]. |
| 968 | Si + LO- 3C-SiC [34]; LO 4H-SiC (964 cm ⁻¹), LO-6H-SiC (965 cm ⁻¹), LO 3C-SiC (972 cm ⁻¹) [14], LO SiC [7], (965 cm ⁻¹) [35]. |

* the frequency 133 cm⁻¹ is closest to the frequency ~ 145 cm⁻¹ of the longitudinal acoustic LA phonons of the 6H-SiC polytype [14].

** In the review paper of S. Kukushkin [7] it was shown that silicon carbide shows three types of vibrational modes on the Raman spectrum:

- longitudinal acoustic LA in the region of low frequencies ~ up to 200 cm⁻¹,
- transverse optical TO at frequencies around 800 cm⁻¹,
- longitudinal-optical LO at frequencies in the region of 900 cm⁻¹.

Doping changes the dynamics of phonons of the matrix structure. For example, doping of zinc sulfide with manganese [36–38], manganese and europium [38] leads to a shift of the phonon frequencies to higher values, blue shifts and anti-Stokes luminescence.

Cheng [39] found the oscillations of the first and the second order phonons on the Raman spectrum of zinc sulfide.

3. Discussion of the results of interpretation of Raman frequencies

In the peak at a frequency of 300 cm^{-1} , the sum of the combined frequencies of CdS + Si+ phosphor based on a solid solution [19].

Genzel [40] theoretically studied the phonon behavior in bulk hexagonal crystals of solid solutions of $\text{Cd}_{1-x}\text{Zn}_x\text{S}$. In the developed model, the difference in the structure of the crystal was not considered, therefore, its use was recommended for analysis of the vibrational LO mode of cubic, hexagonal structures.

Ichimura [41] studied the Raman spectra of bulk crystals of solid solutions of $\text{Cd}_{1-x}\text{Zn}_x\text{S}$ with cubic structure grown on a GaAs substrate. The frequency of vibrational modes with increasing content of Zn shifts to higher values. The frequencies in nanocrystals are shifted to lower values.

In Dorofeev's paper [26], the 517 cm^{-1} line was identified as being related to silicon. The frequencies of silicon are confirmed by Raman spectra for p-Si in the works of Tsu [23], Tsang [24] and for clusters of nc-Si in Ehbrecht [25].

Macias-Sanchez [19] studied micro-Raman spectra of $\text{Cd}_{1-x}\text{Zn}_x\text{S}$ photocatalysts on silicon oxide SBA-16 ($\text{Cd}_{1-x}\text{Zn}_x\text{S}/\text{SBA-16}$). The scattering of light was investigated with the help of the Raman spectrometer Labram-Dior. The source of light was a helium-neon laser with a radiation wavelength $\lambda = 632.8\text{ nm}$ and a power of 15 mW. The spectra were recorded at room temperature in the wave-number range $50\text{--}1100\text{ cm}^{-1}$, the laser spot was focused using a 50x objective. Raman spectra of cadmium sulphide CdS/SBA-16, solid solutions: $\text{Cd}_{0.70}\text{Zn}_{0.30}\text{S}/\text{SBA-16}$, $\text{Cd}_{0.80}\text{Zn}_{0.20}\text{S}/\text{SBA-16}$, $\text{Cd}_{0.90}\text{Zn}_{0.10}\text{S}/\text{SBA-16}$, and $\text{Cd}_{0.95}\text{Zn}_{0.05}\text{S}/\text{SBA-16}$ have been obtained. The Raman spectrum of the samples is represented by frequencies in the region of 300 and 600 cm^{-1} , corresponding to the modes of vibrations of the longitudinally optical phonons of the first 1LO and the second 2LO orders, respectively. A solid solution increases the intensity of 1LO oscillations, especially in the 1LO region of 300 cm^{-1} frequencies. Longitudinal optical oscillations of cadmium sulfide on a CdS/SBA-16 substrate at frequencies of 1LO 300 cm^{-1} and 2LO 600 cm^{-1} are poorly expressed in SBA-16.

Sahoo [16] synthesized by the chemical deposition of nanocrystals of solid solutions of $\text{Cd}_{1-x}\text{Zn}_x\text{S}$ and their structural properties were studied by XRD and Raman spectroscopy. Longitudinal optical (1LO) vibrational modes in $\text{Cd}_{1-x}\text{Zn}_x\text{S}$ nanocrystals have been observed. For nanocrystals, the 1-LO modes turn out to be in the region of lower wavenumbers than bulk ones. The broadening in the spectra of nanocrystals is much larger than in the spectra of bulk crystals. This effect is due to the confinement of phonons. However, in solid substitution solutions, isomorphous substitution makes a much greater contribution to line broadening than the confinement of phonons.

Zakria [42] studied the structural characteristics of thin films of solid solutions $\text{Cd}_{1-x}\text{Zn}_x\text{S}$ $x = 0.2, x = 0.6, x = 0.8$ by X-ray diffraction and Raman spectroscopy for use in optical electronics. The vibrational modes and crystalline phases are investigated. The single-phase hexagonal structure of thin films of solid solutions of $\text{Cd}_{1-x}\text{Zn}_x\text{S}$ was characterized on the Raman spectrum by two vibrational modes 1LO, 2LO. On the Raman spectrum of thin films, after annealing, the red shift and the antisymmetry of the peak corresponding to the vibrational mode as a common blue shift were observed.

Vineeshkumar [43] synthesized quantum dots of phosphors containing copper $\text{Zn}_{1-x-y}\text{Cd}_x\text{Cu}_y\text{S}$ ($x=0.2, y=0, 0.01 \dots 0.1$) at different Cu: Zn ratios, the surface of which is covered by polyvinyl acetate molecules and studied structural, optical and phonon properties, as well as the morphology of the particle surface. The X-ray phase was identified by the XRD method and the particle size in the range $2.5 \dots 3.5$ (nm) was determined.

High-efficiency 3D dimensional photocatalysts Cd_{1-x}Zn_xS were obtained by Z. Xiong [44] in one-stage synthesis and their photocatalytic properties in the decomposition of water molecules by visible light were studied. The phonon properties were studied by Raman spectroscopy. The Raman spectrum of the solid solution Cd_{0.72}Zn_{0.26}S exhibits two peaks at frequencies of 306.5 and 608.1 cm⁻¹.

Analysis of background composition of the Raman spectrum allowed not only to identify the basis of the phosphor film (Figure 2a), but also to confirm the presence of copper and silver in it. Since the joint doping of the solid solution with two Ag + Cu metals changes the phonon dynamics of the structure of solid solutions and leads to additional vibrational modes. This is in agreement with the works of Jimenez-Sandoval [36], Nien [21,37] on the phonon properties of sulfides and the contribution of doping of matrix sulfide to additional modes.

Additional modes (Fig. 2a) are due to the introduction of activators, which cause an oriented distortion of the crystalline cubic face-centered lattice and a decrease in its symmetry [1, 2]. However, it follows from the work of Hossu [38] and Cheng [39] that doping does not affect the frequencies of zinc sulfide of the Raman spectrum, in addition, it was suggested that the frequency of ZnS-sphalerite oscillations should be clarified.

Hossu [38] studied ZnS collation by double-charged Mn²⁺ + Eu²⁺ and showed that the saltification does not change the position of the ZnS peak on the Raman spectrum. Phases ZnS-sphalerite and ZnS-wurtzite were interpreted on the Raman spectrum at frequencies of 350 and 351 cm⁻¹, respectively. Europium increases the luminescence of manganese by 5.5 times. The reason for this effect was explained by the modification of the phonon activity by europium.

As can be seen (Fig. 2a, b), the frequencies of the optical phonons 300 and 522 cm⁻¹ do not change even after the deposition of the polycrystalline phosphor film on the silicon substrate containing the 3C-SiC buffer layer. But this fact does not indicate that the chemical reaction between the polycrystalline Cd_(1-x-y-z) (Cu_yAg_z)Zn_(x)S phosphor film and the substrate of the Si/(nano)SiC heterostructure does not occur. Since a large amount of silicon from the substrate gets into the laser beam of light (Fig. 2a) and a thin surface layer (of the order of a few nanometers), which theoretically could react with the phosphor film, gives a very small contribution in this spectrum, it is very difficult to track. For the same reason, a thin layer of silicon carbide is not visible on the Raman spectrum of the polycrystalline phosphor film (Fig. 2a).

4. Conclusions

Polycrystalline phosphor film Cd_(1-x-y-z) (Cu_yAg_z) Zn_xS was grown on the surface of the Si/nano-SiC heterostructure and different properties of the film were studied: structural, phonon (vibrational), morphology. X-Ray analysis (XRD) showed that the phase composition is represented by a matrix of solid solution of cubic syngony and impurity phases formed during precipitation: sodium sulfate (Na₂SO₄) of orthorhombic syngony and sodium cadmium sulfide (Na₆Cd₇S₁₀) of monoclinic syngony. The Raman spectroscopy (RS) method confirmed the components of the polycrystalline phosphor film. Analysis of the additional Raman bands was conducted, and it was shown, that the doping of the solid solution with copper and silver can affect the optical frequencies, because it distorts the lattice.

Acknowledgments. *A.V. Redkov performed his part of the work with funding of the Russian Science Foundation (grant №19-72-30004). The authors are deeply grateful to Professor S.A Kukushkin for constant attention and useful criticisms. Part of the results was obtained using unique scientific facility "Physics, chemistry, and mechanics of crystals and thin films" (IPME RAS, St. Petersburg).*

References

- [1] Sergeeva NM, Bogdanov SP. Control of optical properties of phosphor $\text{Cd}_{1-x}\text{Zn}_x\text{S}$ containing alloying metals based on copper, silver, manganese. *Optical Journal*. 2017;84(7): 70-79.
- [2] Sergeeva NM, Tsvetkova MN, Bogdanov SP. Influence of sodium chloride on the structural parameters, and spectral-optical properties of Zinc sulfide containing manganese. *Optical Journal*. 2015;82(4): 80-87.
- [3] Lui TY, Zapien JA, Tang H, Ma DDD, Liu YK, Lee CS, Lee ST, Shi SL, Xu SJ. Photoluminescence and photoconductivity properties of copper-doped $\text{Cd}_{1-x}\text{Zn}_x\text{S}$ nanoribbons. *Nanotechnology*. 2006;17(24): 5935-5940.
- [4] Zhu JB, Chang XY, Zhu GJ, Yuan GQ. ZnO.5Cd0.5S Nanocrystals doped with AG2S or CUS: solvothermal synthesis and photoluminescence properties. *Chinese Journal of inorganic chemistry*. 2010;26(12): 2203-2208.
- [5] Gautam NK, Kushwaha K, Kuraria RK, Kuraria SR, Ramrakhiani M. Electroluminescence in $\text{Cd}_{1-x}\text{Zn}_x\text{S}$ Nanocrystals. *International Journal of Luminescence and its applications*. 2014;4(1): 14-16.
- [6] McPeak KM, Opananont B, Shibata T, Ko DK, Becker MA, Chattopadhyay S, Bui HP, Beebe Jr TP, Bunker BA, Murray CB, Baxter JB. Microreactor Chemical Bath Deposition of Laterally Graded $\text{Cd}_{1-x}\text{Zn}_x\text{S}$ Thin Films: A Route to High-Throughput Optimization for Photovoltaic Buffer Layers. *Chemistry of Materials*. 2013;25(3): 297-306.
- [7] Kukushkin SA, Osipov AV. Theory and practice of SiC growth on Si and its applications to wide-gap semiconductor films. *Journal of Physics D: Applied Physics*. 2014;47(31): 313001.
- [8] Kukushkin SA, Osipov AV. New method for growing silicon carbide on silicon by solid-phase epitaxy: Model and experiment. *Physics of the Solid State*. 2008;50(7): 1238-1245.
- [9] Kukushkin SA, Osipov AV. Thin-film heteroepitaxy by the formation of the dilatation dipole ensemble. *Doklady Physics*. 2012;57(5): 217-220.
- [10] Kukushkin SA, Osipov AV. A new method for the synthesis of epitaxial layers of silicon carbide on silicon owing to formation of dilatation dipoles. *Journal of Applied Physics*. 2013;113(2): 4909-1-4909-7.
- [11] Kukushkin SA, Osipov AV, Feoktistov NA. Synthesis of epitaxial silicon carbide films through the substitution of atoms in the silicon crystal lattice: A review. *Physics of the Solid State*. 2014;56(8): 1507-1535.
- [12] Azhniuk YM, Gomonnai AV, Lopushansky VV, Hutyach YI, Turok II, Zahn DRT. Resonant Raman Scattering studies of $\text{Cd}_{1-x}\text{Zn}_x\text{S}$ Nanocrystals. *Journal of Physics: Conference Series*. 2007;92(1): 012044.
- [13] Axtell EA, Kanatzidis MG. Synthesis and Characterization of $\text{Na}_6\text{Cd}_7\text{S}_{10}$: A New Framework Sulfide with 1-D Channels Containing 12- and 16-Member Rings and a Sulfide Anion in an Umbrella-like Geometry. *Chemistry of Materials*. 1996;8(7): 1350-1352.
- [14] Aksyanov IG, Kompan ME, Kulkova IV. Raman scattering of light in silicon carbide mosaic films. *Solid State Physics*. 2010;52(9): 1724-1728.
- [15] Bechelany M, Brioude A, Cornu D, Ferro G, Miele P. A Raman Spectroscopy Study of Individual SiC Nanowires. *Advanced Functional Materials*. 2007;17(6): 939-943.
- [16] Sahoo S, Dhara S, Sivasubramanian V, Kalavathi S, Arora AK. Phonon confinement and substitutional disorder in $\text{Cd}_{1-x}\text{Zn}_x\text{S}$ nanocrystals. *Journal of Raman spectroscopy*. 2009;40(8): 1050-1054.
- [17] Abdi A, Titova LV, Smith LM, Jackson HE, Yarrison-Rice JM, Lensch JL, Lauhon LJ. Resonant Raman scattering from CdS nanowires. *Applied Physics Letters*. 2006;88(4): 043118.

- [18] Antipov VV, Kukushkin SA, Osipov AV. Epitaxial growth of cadmium sulfide films on silicon. *Solid State Physics*. 2016;58(3): 612-615.
- [19] Macias-Sanchez SA, Nava R, Hernandez-Morales V, Acosta-Silva YJ, Pawelec B, Al-Zahrani SM, Navarro RM, Fierro JLG. Cd_{1-x}Zn_xS supported on SBA-16 as photocatalysts for water splitting under visible light: Influence of Zn concentration. *International J. of hydrogen energy*. 2013;38(27): 11799-11810.
- [20] Kukushkin SA, Osipov AV, Redkov AV. Separation of III-N/SiC Epitaxial Heterostructure from a Si Substrate and their Transfer to other Substrate Types. *Semiconductors*. 2017;51(3): 396-401.
- [21] Nien YT, Chen PW, Chen IG. Synthesis and characterization of Zn_{1-x}Cd_xS:Cu, Cl red electroluminescent phosphor powders. *Journal of Alloys and Compounds*. 2008;462(1-2): 398-403.
- [22] Golubev VG, Davydov VY, Medvedev AV, Pevtsov AB, Feoktistov NA. Raman spectra and electrical conductivity of silicon thin films with mixed amorphous-nanocrystalline phase composition: determination of the volume fraction of the nanocrystalline phase. *Solid State Physics*. 1997;39(8): 1348-1353.
- [23] Tsu R, Shen H, Dutta M. Correlation of Raman and photoluminescence spectra of porous silicon. *Applied Physics Letters*. 1992;60(1): 112-114 .
- [24] Tsang JC, Tischler MA, Collins RT. Raman scattering from H or O terminated porous Si. *Applied Physics Letters*. 1992;60(18): 2279-2281.
- [25] Ehbrecht M, Ferkel H, Huisken F, Holz L, Polivanov YN, Smirnov VV, Stelmakh OM, Schmidt R. Deposition and analysis of silicon clusters generated by laser-induced gas phase reaction. *Journal Applied Physics*. 1995;78(9): 5302-5305 .
- [26] Dorofeev SG, Kononov NN, Ishchenko AA, Vasiliev RB, Goldstrakh MA, Zaitseva KV, Koltashev VV, Plotnichenko VG, Tikhonovich OV. Optical and structural properties of thin films deposited from Sol of silicon nanoparticles. *Semiconductors*. 2009;43(11): 1420-1427.
- [27] Davis EA, Lind EL. Physical properties of mixed single crystals of CdS and ZnS. *Journal of Physics and Chemistry of Solids*. 1968;29(1): 79-90.
- [28] Guseva MB, Babayev VG, Khvostov VV, Konyashin IY, Korobov YA, Novikov ND. CVD Diamond with electron conductivity. New Data on FCC-Carbon. *Surface. X-ray, synchrotron and neutron studies*. 2007;10: 22-30.
- [29] Verleur HW, Barker Jr AS. Infrared Lattice Vibrations in GaAs_yP_{1-y} Alloys. *Physical Review*. 1966;149(2): 715-729.
- [30] Verleur HW, Barker Jr AS. Optical Phonons in Mixed Crystals of CdSe_yS_{1-y}. *Physical Review*. 1967;155(3): 750-763.
- [31] Langer DW, Park YS, Euwema RN. Phonon Coupling in Edge Emission and Photoconductivity of CdSe, CdS, and Cd(Se_xS_{1-x}). *Physical Review*. 1966;152(2): 788-796.
- [32] Balkanski M, Beserman M, Besson JM. Phonon processes in mixed crystals of CdS_xCdSe_{1-x}. *Solids State Communications*. 1966;4(5): 201-204.
- [33] Devadoss I, Muthukumaran S, Ashokkumar M. Structural and optical properties of Cd_{1-x}Zn_xS (0 ≤ x ≤ 0.3) nanoparticles. *Journal of Materials Science: Materials in Electronics*. 2014;25(8): 3308-3317.
- [34] Grudinkin SA, Kukushkin SA, Osipov AV, Feoktistov NA. IR spectra of carbon-vacancy clusters at topochemical transformation of silicon into silicon carbide. *Solid State Physics*. 2017;59(12): 2403-2408.
- [35] Nakamoto K. *Infrared and Raman Spectra of Inorganic and Coordination Compounds, Theory and Applications in Inorganic Chemistry, Sixth Edition*. NY: J. Wiley & Sons, Inc.; 2008.

- [36] Jimenez-Sandoval S, Lopez-Rivera A, Irwin JC. Influence of reduced mass differences on the Raman spectra of ternary mixed compounds: $Zn_{1-x}Fe_xS$ and $Zn_{1-x}Mn_xS$. *Physical Review B*. 2003;68(5): 54303.
- [37] Nien YT, Chen IG. Raman scattering and electroluminescence of ZnS:Cu,Cl phosphor powder. *Applied Physics Letters*. 2006;89(26): 261906/3.
- [38] Hossu M, Schaeffer RO, Ma L, Chen W, Zhu Y, Sammynaiken R, Joly AG. On the luminescence enhancement of Mn^{2+} by co-doping of Eu^{2+} in ZnS:Mn,Eu. *Optical Materials*. 2013;35(8): 1513-1519.
- [39] Cheng YC, Jin CQ, Gao F, Wu XL, Zhong W, Li SH, Chu PK. Raman scattering study of zinc blende and wurtzite ZnS. *Journal of Applied Physics*. 2009;106(12): 123505.
- [40] Genzel L, Martin TP, Perry CH. Model for Long - Wavelength Optical - Phonon Modes of Mixed Crystals. *Physica Status Solidi B*. 1974;62(1): 83-92.
- [41] Ichimura M, Usami A, Wada T, Funato M, Ichino K, Fujita Sz, Fujita Sg. Raman spectra of cubic $Zn_{1-x}Cd_xS$. *Physical Review B*. 1992;46(7): 4273-4276.
- [42] Zakria M, Khan TM, Nasir A, Mahmood A. Annealing-induced effects on structural and optical properties of $Cd_{1-x}Zn_xS$ thin films for optoelectronic applications. *Materials Science-Poland*. 2015;33(4): 677-684.
- [43] Vineeshkumar TV, Raj DR, Prasanth S, Sankar P, Unnikrishnan NV, Pillai VPM, Sudarsanakumar C. Composition dependent structural, Raman and nonlinear optical properties of PVA capped $Zn_{1-x-y}Cd_xCu_yS$ Quantum dots. *Optical Materials*. 2016;58: 128-135.
- [44] Xiong Z, Zheng M, Zhu Ch, Zhang B, Ma Li, Shen W. One-step synthesis of highly efficient three-dimensional $Cd_{1-x}Zn_xS$ photocatalysts for visible light photocatalytic water splitting. *Nanoscale Research Letters*. 2013;8(1): 334.